

# Optical nonreciprocity and optomechanical circulator in three-mode optomechanical systems

Xun-Wei Xu<sup>1</sup> and Yong Li<sup>1,2,\*</sup>

<sup>1</sup>Beijing Computational Science Research Center, Beijing 100094, China

<sup>2</sup>Synergetic Innovation Center of Quantum Information and Quantum Physics, University of Science and Technology of China, Hefei, Anhui 230026, China

(Received 5 March 2015; published 28 May 2015)

We demonstrate the possibility of optical nonreciprocal response in a three-mode optomechanical system where one mechanical mode is optomechanically coupled to two linearly coupled optical modes simultaneously. The optical nonreciprocal behavior is induced by the phase difference between the two optomechanical coupling rates, which breaks the time-reversal symmetry of the three-mode optomechanical system. Moreover, the three-mode optomechanical system can also be used as a three-port circulator for two optical modes and one mechanical mode, which we refer to as an optomechanical circulator.

DOI: [10.1103/PhysRevA.91.053854](https://doi.org/10.1103/PhysRevA.91.053854)

PACS number(s): 42.50.Wk, 42.50.Ex, 07.10.Cm, 11.30.Er

## I. INTRODUCTION

The fundamental role of nonreciprocal transmission in information processing has been demonstrated fully by the important application of electrical diodes in electronic information technology with semiconductor *p-n* junctions. However, optical nonreciprocity is constrained by the Lorentz reciprocal theorem due to the time-reversal symmetry in linear and nonmagnetic media [1]. Traditionally, optical nonreciprocity is based on magneto-optical crystals [2] by breaking the time-reversal symmetry with the Faraday rotation effect or optical nonlinear systems [3] by circumventing the symmetrical constraint. Recently, a number of alternative schemes based on diverse mechanisms have been proposed, such as spatial-symmetry-breaking structures [4], indirect interband photonic transitions [5], optoacoustic effects [6], parity-time-symmetric structures [7], and moving systems [8]. Moreover, for the potential applications in photonic quantum information processing, the abilities to be integrated on a chip and operated on a single-photon level [9] are desirable features for the realization of nonreciprocal photonic devices in the future.

With rapidly growing interest as a new class of microscale integrable devices, optomechanical systems have shown enormous potential for application in quantum information processing [10]. It has already been shown that optomechanical systems can be used to induce nonreciprocal effects for light [11,12]. At the beginning, the optical nonreciprocal effect was based on the momentum difference between forward- and backward-moving light beams in an optomechanical system consisting of an in-line Fabry-Pérot cavity with one movable mirror and one fixed mirror [11]. Subsequently, a new approach for a nonreciprocal optomechanical device was proposed by using strong optomechanical interaction in microring resonators [12]. The nonreciprocal response is obtained when the optomechanical coupling is enhanced in one direction and suppressed in the other one by optically pumping the ring resonator. In principle, the scheme shown in Ref. [12] can be applied on a single-photon level, in spite of the limitation induced by the up-conversion of thermal phonons.

We note that besides the standard optomechanics with an optical cavity mode coupled to a mechanical mode through the radiation pressure interaction, three-mode optomechanical systems including two optical modes coupled to one mechanical mode have drawn much attention recently. Some interesting phenomena are found in three-mode optomechanical systems, such as enhanced quantum nonlinearities [13], high-fidelity quantum state transfer [14], phonon lasing [15], motional ground-state cooling in the unresolved sideband regime [16], and unconventional photon blockade [17].

In this paper, we propose a scheme for optical nonreciprocity in a three-mode optomechanical system, where two optical modes are linearly coupled to each other and one mechanical mode is optomechanically coupled to the two optical modes simultaneously. The two effective optomechanical couplings are both enhanced by pumping the two optical modes with different external driving fields. Most crucially, there is a phase difference between the two effective optomechanical couplings, which cannot be absorbed into local redefinitions of the operators. Nonreciprocal response of the three-mode optomechanical system is induced by this phase difference, which is gauge invariant and is associated with the time-reversal symmetry broken for the three-mode system [18,19]. This mechanism has been used in the circuit-QED architecture [18] and phonon devices [19] for breaking time-reversal symmetry, and photon or phonon circulator behavior [18,19] was predicted accordingly. Thus, the present three-mode optomechanical system can also be used as a three-port circulator formed by two optical modes and one mechanical mode, which we refer to as optomechanical circulator. This type of circulator may serve as a suitable interface for the hybrid network composed of optical (or microwave) and mechanical systems.

This paper is organized as follows: In Sec. II, the Hamiltonian of a three-mode optomechanical system is introduced, and the spectra of the output fields are obtained formally. The optical nonreciprocal response is shown in Sec. III, and the optomechanical circulator behavior is discussed in Sec. IV. Finally, we draw our conclusions in Sec. V.

## II. MODEL

We consider a three-mode optomechanical system consisting of two optical modes (*a* and *b*, frequencies  $\omega_a$  and  $\omega_b$ ) and

\*liyong@csirc.ac.cn

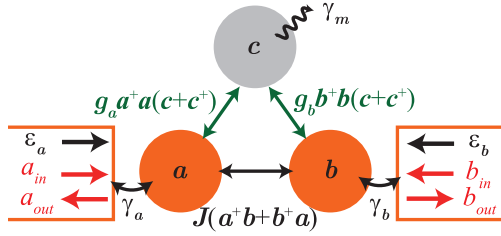


FIG. 1. (Color online) Schematic diagram of an optomechanical system consisting of two optical modes ( $a$  and  $b$ ) and one mechanical mode ( $c$ ). The optical modes and the mechanical mode are coupled via radiation pressure; meanwhile, the two optical modes are linearly coupled to each other.

one mechanical mode ( $c$ , frequency  $\omega_m$ ) as shown in Fig. 1. The optomechanical coupling rates between the optical modes and the mechanical mode are denoted by  $g_a$  and  $g_b$ ; two optical modes are linearly coupled mutually at rate  $J$  and driven by external laser sources with frequencies  $\omega_{a,d} = \omega_{b,d} = \omega_d$  at rates  $\varepsilon_a$  and  $\varepsilon_b$ , respectively. The Hamiltonian of the system in the rotating frame at the frequency of the driving fields  $\omega_d$  is

$$\begin{aligned} H = & \hbar\Delta_a a^\dagger a + \hbar\Delta_b b^\dagger b + \hbar\omega_m c^\dagger c + \hbar J(a^\dagger b + ab^\dagger) \\ & + \hbar g_a a^\dagger a(c + c^\dagger) + \hbar g_b b^\dagger b(c + c^\dagger) \\ & + i\hbar(\varepsilon_a a^\dagger e^{i\phi_a} + \varepsilon_b b^\dagger e^{i\phi_b} - \text{H.c.}), \end{aligned} \quad (1)$$

where  $\Delta_a = \omega_a - \omega_d$  and  $\Delta_b = \omega_b - \omega_d$  are the detunings between the optical modes and the driving fields. Without loss of generality, we assume that  $J$ ,  $\varepsilon_a$ , and  $\varepsilon_b$  are real, and  $\phi_a$  ( $\phi_b$ ) is the phase of the laser field coupling to optical mode  $a$  ( $b$ ). This kind of Hamiltonian can be realized in the optomechanical system with a membrane in a Fabry-Pérot cavity [20], microtoroid optomechanical cavities [21], optomechanical crystals [22], and electromechanical devices [23].

Substituting the Hamiltonian (1) into the Heisenberg equation and taking into account the damping and corresponding noise terms, we get the quantum Langevin equations (QLEs) for the operators of the optical and mechanical modes:

$$\begin{aligned} \frac{d}{dt}a = & \left\{-\frac{\gamma_a}{2} - i[\Delta_a + g_a(c + c^\dagger)]\right\}a - iJa \\ & + \varepsilon_a e^{i\phi_a} + \sqrt{\gamma_a}a_{\text{in}}, \end{aligned} \quad (2)$$

$$\begin{aligned} \frac{d}{dt}b = & \left\{-\frac{\gamma_b}{2} - i[\Delta_b + g_b(c + c^\dagger)]\right\}b - iJa \\ & + \varepsilon_b e^{i\phi_b} + \sqrt{\gamma_b}b_{\text{in}}, \end{aligned} \quad (3)$$

$$\frac{d}{dt}c = \left(-\frac{\gamma_m}{2} - i\omega_m\right)c - i(g_a a^\dagger a + g_b b^\dagger b) + \sqrt{\gamma_m}c_{\text{in}}. \quad (4)$$

Here  $\gamma_a$  ( $\gamma_b$ ) is the damping rate of optical mode  $a$  ( $b$ ), and  $\gamma_m$  is the mechanical damping rate.  $a_{\text{in}}$ ,  $b_{\text{in}}$ , and  $c_{\text{in}}$  are the input quantum fields with zero mean values, and the spectra of the input quantum fields  $s_{v,\text{in}}(\omega)$  are defined via  $\langle v_{\text{in}}^\dagger(\omega')\widetilde{v}_{\text{in}}(\omega) \rangle = s_{v,\text{in}}(\omega)\delta(\omega + \omega')$  and  $\langle \widetilde{v}_{\text{in}}(\omega')v_{\text{in}}^\dagger(\omega) \rangle = [1 + s_{v,\text{in}}(\omega)]\delta(\omega + \omega')$ , where the term 1 results from the

effect of vacuum noise and  $v_{\text{in}}^\dagger$  ( $\widetilde{v}_{\text{in}}$ ) is the Fourier transform of  $v_{\text{in}}^\dagger$  ( $v_{\text{in}}$ ) for  $v = a, b, c$ .

The mean values of the operators in the steady state can be obtained from the nonlinear QLEs (2)–(4) by using a factorization assumption like  $\langle ca \rangle = \langle c \rangle \langle a \rangle$ , and then

$$\langle a \rangle = \alpha = \frac{\left(\frac{\gamma_b}{2} + i\Delta'_b\right)\varepsilon_a e^{i\phi_a} - iJ\varepsilon_b e^{i\phi_b}}{\left(\frac{\gamma_a}{2} + i\Delta'_a\right)\left(\frac{\gamma_b}{2} + i\Delta'_b\right) + J^2}, \quad (5)$$

$$\langle b \rangle = \beta = \frac{\left(\frac{\gamma_a}{2} + i\Delta'_a\right)\varepsilon_b e^{i\phi_b} - iJ\varepsilon_a e^{i\phi_a}}{\left(\frac{\gamma_a}{2} + i\Delta'_a\right)\left(\frac{\gamma_b}{2} + i\Delta'_b\right) + J^2}, \quad (6)$$

$$\langle c \rangle = \xi = \frac{-i(g_a|\alpha|^2 + g_b|\beta|^2)}{\left(\frac{\gamma_m}{2} + i\omega_m\right)}, \quad (7)$$

where  $\Delta'_a = \Delta_a + g_a(\xi + \xi^*)$  and  $\Delta'_b = \Delta_b + g_b(\xi + \xi^*)$  are the effective detunings including the frequency shifts caused by the optomechanical interaction.

To solve the nonlinear QLEs (2)–(4), the operators are rewritten as the sum of the mean values and the small quantum fluctuation terms, i.e.,  $a = \alpha + \delta a$ ,  $b = \beta + \delta b$ ,  $c = \xi + \delta c$ . When the driving fields are strong enough that  $\delta a \ll |\alpha|$  and  $\delta b \ll |\beta|$ , then we can linearize the equations by neglecting the high-order small terms. Substituting them into the nonlinear QLEs (2)–(4) and keeping only the first-order terms in the small quantum fluctuation terms  $\delta a$ ,  $\delta b$ , and  $\delta c$ , we obtain the linearized QLEs:

$$\begin{aligned} \frac{d}{dt}\delta a = & \left(-\frac{\gamma_a}{2} - i\Delta'_a\right)\delta a - iG_a(\delta c + \delta c^\dagger) \\ & - iJ\delta b + \sqrt{\gamma_a}a_{\text{in}}, \end{aligned} \quad (8)$$

$$\begin{aligned} \frac{d}{dt}\delta b = & \left(-\frac{\gamma_b}{2} - i\Delta'_b\right)\delta b - iG_b(\delta c + \delta c^\dagger) \\ & - iJ\delta a + \sqrt{\gamma_b}b_{\text{in}}, \end{aligned} \quad (9)$$

$$\begin{aligned} \frac{d}{dt}\delta c = & \left(-\frac{\gamma_m}{2} - i\omega_m\right)\delta c - i(G_a\delta a^\dagger + G_a^*\delta a) \\ & - i(G_b\delta b^\dagger + G_b^*\delta b) + \sqrt{\gamma_m}c_{\text{in}}, \end{aligned} \quad (10)$$

where  $G_a = g_a\alpha = |G_a|e^{i\theta_a}$  and  $G_b = g_b\beta = |G_b|e^{i\theta_b}$  are the effective optomechanical coupling rates with phase difference  $\theta \equiv \theta_b - \theta_a$ . Actually, the phase of  $G_a$  (or  $G_b$ ) can be absorbed into new redefinitions of the operators  $\delta a$  and  $\delta b$ , and only the phase difference  $\theta$  has physical effects. Without loss of generality,  $G_a$  is assumed to be real in the following numerical calculations.

For convenience, the linearized QLEs (8)–(10) can be concisely expressed as

$$\frac{d}{dt}V = -MV + \Gamma V_{\text{in}}, \quad (11)$$

where the fluctuation vector  $V = (\delta a, \delta b, \delta c, \delta a^\dagger, \delta b^\dagger, \delta c^\dagger)^T$ , the input field vector  $V_{\text{in}} = (a_{\text{in}}, b_{\text{in}}, c_{\text{in}}, a_{\text{in}}^\dagger, b_{\text{in}}^\dagger, c_{\text{in}}^\dagger)^T$ ,  $\Gamma = \text{diag}(\sqrt{\gamma_a}, \sqrt{\gamma_b}, \sqrt{\gamma_m}, \sqrt{\gamma_a}, \sqrt{\gamma_b}, \sqrt{\gamma_m})$  denotes the damping

matrix, and  $M$  is the coefficient matrix

$$M = \begin{pmatrix} \frac{\gamma_a}{2} + i\Delta'_a & iJ & iG_a & 0 & 0 & iG_a \\ iJ & \frac{\gamma_b}{2} + i\Delta'_b & iG_b & 0 & 0 & iG_b \\ iG_a^* & iG_b^* & \frac{\gamma_m}{2} + i\omega_m & iG_a & iG_b & 0 \\ 0 & 0 & -iG_a^* & \frac{\gamma_a}{2} - i\Delta'_a & -iJ & -iG_a^* \\ 0 & 0 & -iG_b^* & -iJ & \frac{\gamma_b}{2} - i\Delta'_b & -iG_b^* \\ -iG_a^* & -iG_b^* & 0 & -iG_a & -iG_b & \frac{\gamma_m}{2} - i\omega_m \end{pmatrix}. \quad (12)$$

The system is stable only if the real parts of all the eigenvalues of matrix  $M$  are positive. The stability conditions can be given explicitly by using the Routh-Hurwitz criterion [24]. However, they are too cumbersome to be given here. In the following discussions, we make sure the stability conditions are satisfied for the used parameters.

By introducing the Fourier transform of the operators

$$\tilde{o}(\omega) = \frac{1}{\sqrt{2\pi}} \int_{-\infty}^{+\infty} o(t)e^{i\omega t} dt, \quad (13)$$

$$\tilde{o}^\dagger(\omega) = \frac{1}{\sqrt{2\pi}} \int_{-\infty}^{+\infty} o^\dagger(t)e^{i\omega t} dt \quad (14)$$

(for any operator  $o$ ) and using the properties of Fourier transformation, the solution to the linearized QLEs (11) in the frequency domain is

$$\tilde{V}(\omega) = (M - i\omega I)^{-1} \Gamma \tilde{V}_{\text{in}}(\omega), \quad (15)$$

where  $I$  denotes the identity matrix.

As a consequence of boundary conditions, the relation among the input, internal, and output fields is given as [25]

$$v_{\text{out}} + v_{\text{in}} = \sqrt{\gamma_v} \delta v \quad (16)$$

for  $v = a, b, c$  and  $\gamma_c \equiv \gamma_m$ . Then the output field vector in the frequency domain is

$$\tilde{V}_{\text{out}}(\omega) = U(\omega) \tilde{V}_{\text{in}}(\omega), \quad (17)$$

where the output field vector  $\tilde{V}_{\text{out}}(\omega)$  is the Fourier transform of  $V_{\text{out}} = (a_{\text{out}}, b_{\text{out}}, c_{\text{out}}, a_{\text{out}}^\dagger, b_{\text{out}}^\dagger, c_{\text{out}}^\dagger)^T$  and

$$U(\omega) = \Gamma(M - i\omega I)^{-1} \Gamma - I. \quad (18)$$

The spectrum of the output fields is defined by

$$s_{v,\text{out}}(\omega) = \int d\omega' \langle \tilde{v}_{\text{out}}^\dagger(\omega') \tilde{v}_{\text{out}}(\omega) \rangle. \quad (19)$$

By substituting the expression of  $\tilde{V}_{\text{out}}(\omega)$  [Eq. (17)] into Eq. (19), one can obtain [26]

$$S_{\text{out}}(\omega) = T(\omega) S_{\text{in}}(\omega) + S_{\text{vac}}(\omega). \quad (20)$$

Here  $S_{\text{in}}(\omega) = (s_{a,\text{in}}(\omega), s_{b,\text{in}}(\omega), s_{c,\text{in}}(\omega))^T$ ,  $S_{\text{out}}(\omega) = (s_{a,\text{out}}(\omega), s_{b,\text{out}}(\omega), s_{c,\text{out}}(\omega))^T$ ,  $S_{\text{vac}}(\omega) = (s_{a,\text{vac}}(\omega), s_{b,\text{vac}}(\omega), s_{c,\text{vac}}(\omega))^T$ , and

$$T(\omega) = \begin{pmatrix} T_{aa}(\omega) & T_{ab}(\omega) & T_{ac}(\omega) \\ T_{ba}(\omega) & T_{bb}(\omega) & T_{bc}(\omega) \\ T_{ca}(\omega) & T_{cb}(\omega) & T_{cc}(\omega) \end{pmatrix}, \quad (21)$$

where the element  $T_{ij}(\omega)$  ( $i, j = a, b, c$ ) denotes the scattering probability that corresponds to the output field of mode  $i$  arising from the presence of a single photon (or single phonon) in the input field of mode  $j$ . The scattering probabilities are given as

$$T_{aa}(\omega) = |U_{11}(\omega)|^2 + |U_{14}(\omega)|^2, \quad (22)$$

$$T_{ab}(\omega) = |U_{12}(\omega)|^2 + |U_{15}(\omega)|^2, \quad (23)$$

$$T_{ac}(\omega) = |U_{13}(\omega)|^2 + |U_{16}(\omega)|^2, \quad (24)$$

$$T_{ba}(\omega) = |U_{21}(\omega)|^2 + |U_{24}(\omega)|^2, \quad (25)$$

$$T_{bb}(\omega) = |U_{22}(\omega)|^2 + |U_{25}(\omega)|^2, \quad (26)$$

$$T_{bc}(\omega) = |U_{23}(\omega)|^2 + |U_{26}(\omega)|^2, \quad (27)$$

$$T_{ca}(\omega) = |U_{31}(\omega)|^2 + |U_{34}(\omega)|^2, \quad (28)$$

$$T_{cb}(\omega) = |U_{32}(\omega)|^2 + |U_{35}(\omega)|^2, \quad (29)$$

$$T_{cc}(\omega) = |U_{33}(\omega)|^2 + |U_{36}(\omega)|^2, \quad (30)$$

where  $U_{ij}(\omega)$  (for  $i, j = 1, \dots, 6$ ) represents the element at the  $i$ th row and  $j$ th column of the matrix  $U(\omega)$  given by Eq. (18).  $s_{v,\text{vac}}$  ( $v = a, b, c$ ) is the output spectrum contributing from the input vacuum field,

$$s_{a,\text{vac}}(\omega) = |U_{14}(\omega)|^2 + |U_{15}(\omega)|^2 + |U_{16}(\omega)|^2, \quad (31)$$

$$s_{b,\text{vac}}(\omega) = |U_{24}(\omega)|^2 + |U_{25}(\omega)|^2 + |U_{26}(\omega)|^2, \quad (32)$$

$$s_{c,\text{vac}}(\omega) = |U_{34}(\omega)|^2 + |U_{35}(\omega)|^2 + |U_{36}(\omega)|^2. \quad (33)$$

### III. OPTICAL NONRECIPROCITY

In this and the next sections, we numerically evaluate the scattering probabilities to show the possibility of optical nonreciprocal response and optomechanical circulator behavior in the three-mode optomechanical system. The optimal parameters for the observation of optical nonreciprocal response are obtained according to the numerical results. The physical origin of the optical nonreciprocal response and optomechanical circulator behavior will be discussed in the next section.

Scattering probabilities  $T_{ab}(\omega)$  and  $T_{ba}(\omega)$  as functions of the frequency of the incoming signal  $\omega$  for different phase differences are shown in Fig. 2, where the parameters are  $\Delta'_a = \Delta'_b = \omega_m = 10\gamma$ ,  $J = G_a = G_b e^{-i\theta} = \gamma_a/2 = \gamma_b/2 = \gamma_m/2 = \gamma/2$ . The photon transmission satisfies the Lorentz reciprocal theorem [e.g.,  $T_{ab}(\omega) = T_{ba}(\omega)$ ] on the condition that  $\theta = 0$  or  $\pi$ . When  $\theta \neq n\pi$  ( $n$  is an integer), the time-reversal symmetry is broken, and the three-mode optomechanical system exhibits a nonreciprocal response. In

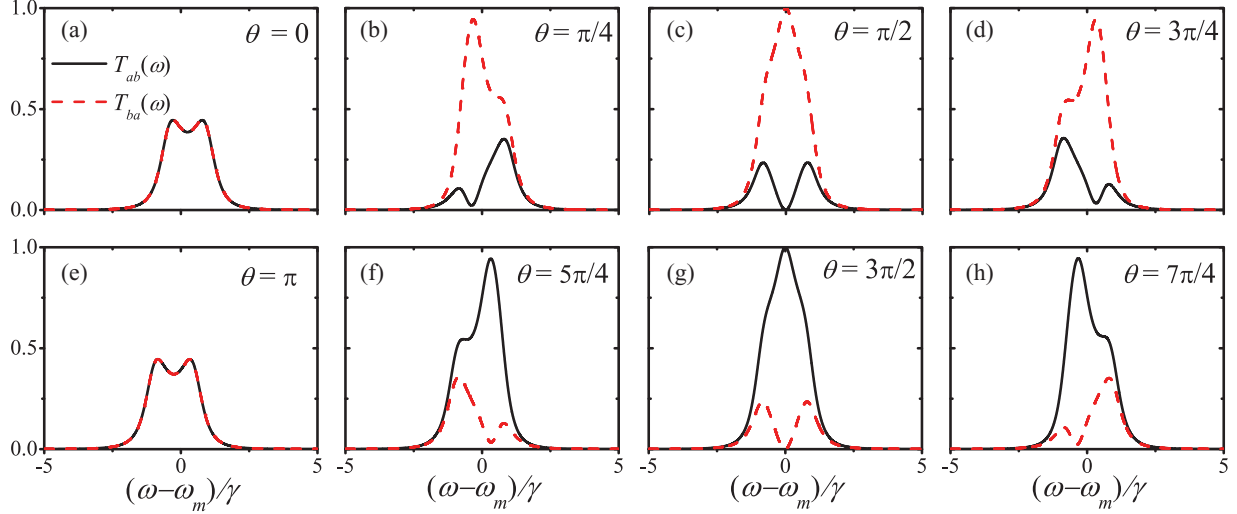


FIG. 2. (Color online) Scattering probabilities  $T_{ab}(\omega)$  (black solid lines) and  $T_{ba}(\omega)$  (red dashed lines) as functions of the frequency of the incoming signal  $\omega$  for different phase difference: (a)  $\theta = 0$ , (b)  $\theta = \pi/4$ , (c)  $\theta = \pi/2$ , (d)  $\theta = 3\pi/4$ , (e)  $\theta = \pi$ , (f)  $\theta = 5\pi/4$ , (g)  $\theta = 3\pi/2$ , and (h)  $\theta = 7\pi/4$ . The other parameters are  $\Delta'_a = \Delta'_b = \omega_m = 10\gamma$ ,  $J = G_a = G_b e^{-i\theta} = \gamma_a/2 = \gamma_b/2 = \gamma_m/2 = \gamma/2$ .

the regime  $0 < \theta < \pi$ , we have  $T_{ab}(\omega) < T_{ba}(\omega)$ ; in the regime  $\pi < \theta < 2\pi$ , we have  $T_{ab}(\omega) > T_{ba}(\omega)$ . The optimal optical nonreciprocal response is obtained as  $\theta = \pi/2$  [ $T_{ab}(\omega) \approx 0$  and  $T_{ba}(\omega) \approx 1$  at  $\omega = \omega_m$ ] and  $\theta = 3\pi/2$  [ $T_{ab}(\omega) \approx 1$  and  $T_{ba}(\omega) \approx 0$  at  $\omega = \omega_m$ ]. The condition of  $G_a = G_b e^{-i\theta} = \gamma/2$  with  $g_a = g_b = g$  can be obtained approximately by setting the amplitudes and the phases of the coupling laser fields as

$$\varepsilon_a = \varepsilon_b \approx \frac{\gamma \omega_m}{2g}, \quad (34)$$

$$\phi_a = \phi_b - \theta \approx \frac{\pi}{2}. \quad (35)$$

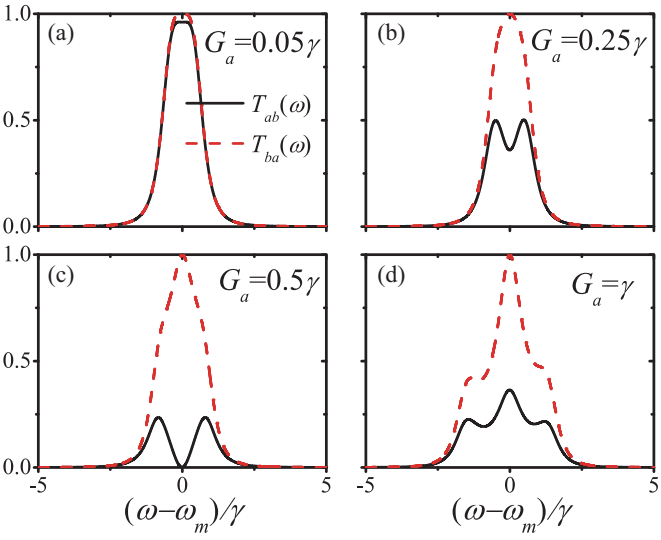


FIG. 3. (Color online) Scattering probabilities  $T_{ab}(\omega)$  (black solid line) and  $T_{ba}(\omega)$  (red dashed line) as functions of the frequency of the incoming signal  $\omega$  for different effective optomechanical coupling rates: (a)  $G_a = 0.05\gamma$ , (b)  $G_a = 0.25\gamma$ , (c)  $G_a = 0.5\gamma$ , and (d)  $G_a = \gamma$ . The other parameters are  $\Delta'_a = \Delta'_b = \omega_m = 10\gamma$ ,  $J = \gamma_a/2 = \gamma_b/2 = \gamma_m/2 = \gamma/2$ . Here we fix  $G_b = iG_a$ , which corresponds to the case of  $\theta = \pi/2$ .

In Fig. 3, the scattering probabilities  $T_{ab}(\omega)$  and  $T_{ba}(\omega)$  are shown as functions of the frequency of the incoming signal  $\omega$  for different effective optomechanical coupling rates  $G_a$  with the parameters  $\Delta'_a = \Delta'_b = \omega_m = 10\gamma$ ,  $J = \gamma_a/2 = \gamma_b/2 = \gamma_m/2 = \gamma/2$ ,  $G_b = iG_a$ . It is shown that as the effective optomechanical coupling is weak ( $|G_a|, |G_b| \ll \gamma$ ), the scattering probability from mode  $b$  to mode  $a$  is almost the same as the one from mode  $a$  to mode  $b$ , e.g.,  $T_{ab}(\omega) \approx T_{ba}(\omega)$ . With the enhancement of the effective optomechanical coupling rates, the optical nonreciprocal response becomes obvious and reaches the optimal effect at about  $G_a = 0.5\gamma$ .

In Fig. 4, we plot the scattering probabilities  $T_{ab}(\omega)$  and  $T_{ba}(\omega)$  for different mechanical damping rates  $\gamma_m$  with the pa-

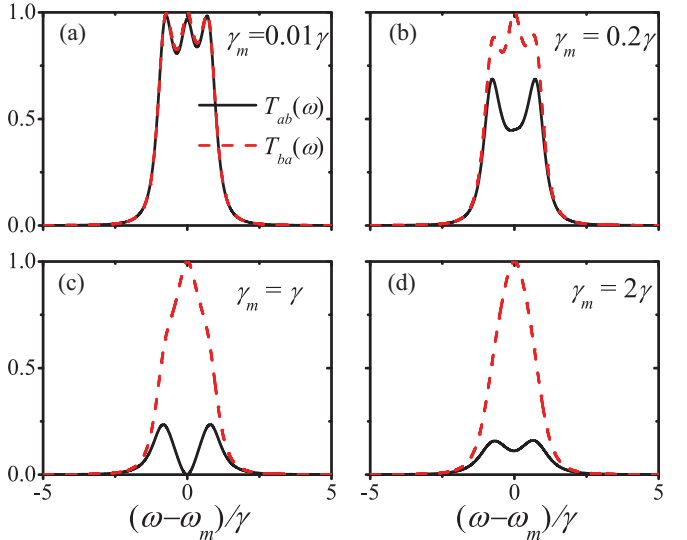


FIG. 4. (Color online) Scattering probabilities  $T_{ab}(\omega)$  (black solid lines) and  $T_{ba}(\omega)$  (red dashed lines) as functions of the frequency of the incoming signal  $\omega$  for different mechanical damping rates: (a)  $\gamma_m = 0.01\gamma$ , (b)  $\gamma_m = 0.2\gamma$ , (c)  $\gamma_m = \gamma$ , and (d)  $\gamma_m = 2\gamma$ . The other parameters are  $\Delta'_a = \Delta'_b = \omega_m = 10\gamma$ ,  $J = G_a = -iG_b = \gamma_a/2 = \gamma_b/2 = \gamma/2$ .

rameters  $\Delta'_a = \Delta'_b = \omega_m = 10\gamma$ ,  $J = G_a = -iG_b = \gamma_a/2 = \gamma_b/2 = \gamma/2$ . It is shown that as the mechanical damping rate  $\gamma_m$  is much smaller than the optical damping rate ( $\gamma_m \ll \gamma$ ), the photon scattering probabilities are almost the same for the two directions, e.g.  $T_{ab}(\omega) \approx T_{ba}(\omega)$ . With the increase of the mechanical damping rate, the optical nonreciprocal response becomes obvious and achieves the optimal effect for  $\gamma_m \approx \gamma$ .

#### IV. OPTOMECHANICAL CIRCULATOR

As done in most studies on optomechanical systems, the signals input and output from the mechanical mode were not considered in the last section. With the development of phonon-based systems, the phonon is another useful medium for quantum information processing. The propagation of phonons can be efficiently controlled by means of periodic patterning of materials (phononic crystals), and the phonon waveguides based on phononic-crystal structures provide a very promising and versatile platform for realizing phonon-state transmission [27]. Recently, a two-dimensional structure of the optomechanical crystal has been designed to trap optical and acoustic oscillations together and to enhance the strength of phonon-photon interaction [22]. Phonon-photon translators and phonon routers for phononic quantum networks were also proposed based on the coupled photonic and phononic crystals [19,28]. With these developments, we assume in this section that the mechanical mode is coupled to a continuous mode of the phonon waveguide and the phonons can be input and output through the phonon waveguide. The scattering of both photons and phonons in the three-mode optomechanical system is considered in the following.

Using Eqs. (22)–(30), we now show the numerical results of all the scattering probabilities (nine elements) in Eqs. (21). As shown in Fig. 5, the three-mode optomechanical system shows circulator behavior: when  $\theta = \pi/2$ , we have  $T_{ba}(\omega) \approx T_{cb}(\omega) \approx T_{ac}(\omega) \approx 1$  and the other scattering probabilities equal to zero at  $\omega = \omega_m$ , as shown in Figs. 5(a), 5(c), and 5(e); when  $\theta = 3\pi/2$ , we have  $T_{ca}(\omega) \approx T_{ab}(\omega) \approx T_{bc}(\omega) \approx 1$  and the other scattering probabilities equal to zero at  $\omega = \omega_m$ , as shown in Figs. 5(b), 5(d), and 5(f). That is to say, the signal is transferred from one mode to another in either a counterclockwise ( $a \rightarrow b \rightarrow c \rightarrow a$ ) or clockwise ( $a \rightarrow c \rightarrow b \rightarrow a$ ) direction, depending on the relative phase  $\theta = \pi/2$  or  $3\pi/2$ , as shown in Fig. 6.

The scattering matrix for the optomechanical circulator in three-mode optomechanical systems can be obtained analytically, similar to the case for photon and phonon circulators in Refs. [18,19]. We assume that  $\omega_m \approx \Delta \gg \{J, |G_a|, |G_b|, \gamma_a, \gamma_b, \gamma_m\}$ ; then Eqs. (8)–(10) can be simplified by the rotating-wave approximation as

$$\frac{d}{dt}\delta a = \left(-\frac{\gamma_a}{2} - i\Delta'_a\right)\delta a - iG_a\delta c - iJ\delta b + \sqrt{\gamma_a}a_{in}, \quad (36)$$

$$\frac{d}{dt}\delta b = \left(-\frac{\gamma_b}{2} - i\Delta'_b\right)\delta b - iG_b\delta c - iJ\delta a + \sqrt{\gamma_b}b_{in}, \quad (37)$$

$$\frac{d}{dt}\delta c = \left(-\frac{\gamma_m}{2} - i\omega_m\right)\delta c - iG_a^*\delta a - iG_b^*\delta b + \sqrt{\gamma_m}c_{in}. \quad (38)$$

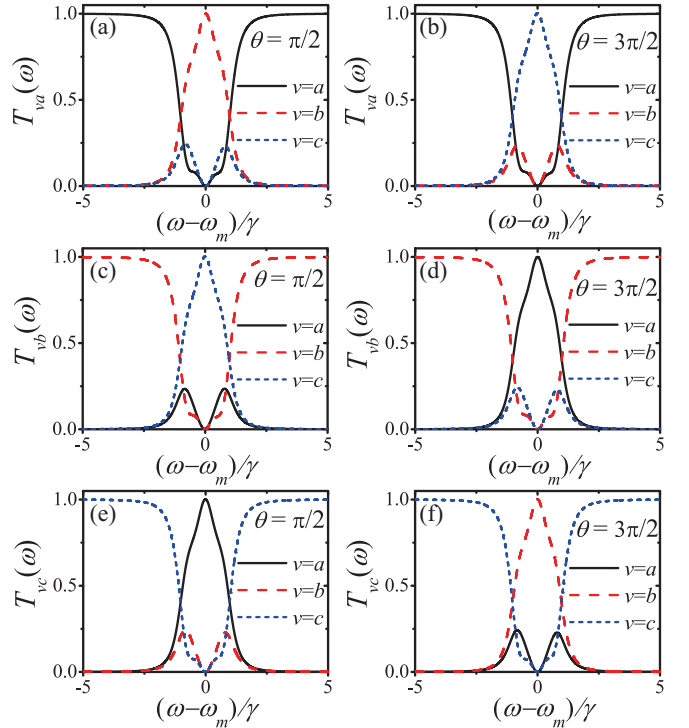


FIG. 5. (Color online) Scattering probabilities (a) and (b)  $T_{va}(\omega)$ , (c) and (d)  $T_{vb}(\omega)$  and (e) and (f)  $T_{vc}(\omega)$  ( $v = a, b, c$ ) as functions of the frequency of the incoming signal  $\omega$  for different phase difference: (a), (c), and (e)  $\theta = \pi/2$ ; (b), (d), and (f)  $\theta = 3\pi/2$ . The other parameters are  $\Delta'_a = \Delta'_b = \omega_m = 10\gamma$ ,  $J = G_a = G_b e^{-i\theta} = \gamma_a/2 = \gamma_b/2 = \gamma_m/2 = \gamma/2$ .

Thus, the effective Hamiltonian after linearization takes the form (the effective system is shown in Fig. 6)

$$H_{\text{eff}} = \hbar\Delta'_a a^\dagger a + \hbar\Delta'_b b^\dagger b + \hbar\omega_m c^\dagger c + \hbar(Jb^\dagger a + |G_a|e^{i\theta_a}a^\dagger c + |G_b|e^{-i\theta_b}c^\dagger b + \text{H.c.}) \quad (39)$$

The necessary and sufficient condition of time-reversal symmetry is that the gauge-invariant phase sum is an integral multiple of  $\pi$  [18]. Thus, for the present Hamiltonian (39), we need

$$\theta_b - \theta_a \equiv \theta = n\pi \quad (40)$$

for real  $J$ , where  $n$  is an integral number [also see the numerical results shown in Figs. 2(a) and 2(e)]. The optical

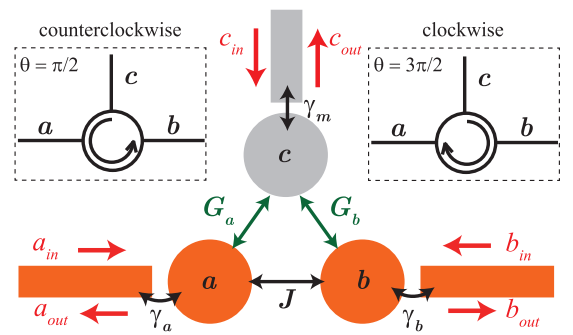


FIG. 6. (Color online) Schematic diagram of a three-mode optomechanical circulator.

nonreciprocal response and the optomechanical circulator behavior are induced by breaking the time-reversal symmetry (i.e.,  $\theta_b - \theta_a \neq n\pi$ ), and the optimal effect is realized halfway between the time-reversal-symmetric points (i.e.,  $\theta_a = 0, \theta_b = \theta = \pi/2$  or  $3\pi/2$ ), as shown in Fig. 5.

Now we will derive the scattering matrix of the optomechanical circulator behavior analytically from the simplified linearized QLEs [Eqs. (36)–(38)]. Let us transform the linearized equations into the frequency domain,

$$(M' - i\omega I) \begin{pmatrix} \tilde{\delta a} \\ \tilde{\delta b} \\ \tilde{\delta c} \end{pmatrix} = \begin{pmatrix} \sqrt{\gamma_a} \tilde{a}_{in} \\ \sqrt{\gamma_b} \tilde{b}_{in} \\ \sqrt{\gamma_m} \tilde{c}_{in} \end{pmatrix}, \quad (41)$$

where

$$M' = \begin{pmatrix} \frac{\gamma_a}{2} + i\Delta'_a & iJ & iG_a \\ iJ & \frac{\gamma_b}{2} + i\Delta'_b & iG_b \\ iG_a^* & iG_b^* & \frac{\gamma_m}{2} + i\omega_m \end{pmatrix}. \quad (42)$$

In the conditions for the optimal optomechanical circulator, i.e.,  $\omega = \Delta'_a = \Delta'_b = \omega_m$  and  $J = G_a = G_b e^{-i\theta} = \gamma_a/2 = \gamma_b/2 = \gamma_m/2 = \gamma/2$ , we have

$$\frac{\gamma}{2} \begin{pmatrix} 1 & i & i \\ i & 1 & i e^{i\theta} \\ i & i e^{-i\theta} & 1 \end{pmatrix} \begin{pmatrix} \tilde{\delta a} \\ \tilde{\delta b} \\ \tilde{\delta c} \end{pmatrix} = \begin{pmatrix} \sqrt{\gamma} \tilde{a}_{in} \\ \sqrt{\gamma} \tilde{b}_{in} \\ \sqrt{\gamma} \tilde{c}_{in} \end{pmatrix}. \quad (43)$$

By choosing  $\theta = \pi/2$ , the scattering matrix is given through

$$\begin{pmatrix} \tilde{a}_{out} \\ \tilde{b}_{out} \\ \tilde{c}_{out} \end{pmatrix} = \begin{pmatrix} 0 & 0 & -i \\ -i & 0 & 0 \\ 0 & -1 & 0 \end{pmatrix} \begin{pmatrix} \tilde{a}_{in} \\ \tilde{b}_{in} \\ \tilde{c}_{in} \end{pmatrix}. \quad (44)$$

By choosing  $\theta = 3\pi/2$ , we can get the scattering matrix through

$$\begin{pmatrix} \tilde{a}_{out} \\ \tilde{b}_{out} \\ \tilde{c}_{out} \end{pmatrix} = \begin{pmatrix} 0 & -i & 0 \\ 0 & 0 & -1 \\ -i & 0 & 0 \end{pmatrix} \begin{pmatrix} \tilde{a}_{in} \\ \tilde{b}_{in} \\ \tilde{c}_{in} \end{pmatrix}. \quad (45)$$

Equation (44) clearly shows a perfect circulator with the signal transferring counterclockwise ( $a \rightarrow b \rightarrow c \rightarrow a$ ) for  $\theta = \pi/2$ , and Eq. (45) describes an ideal circulator with the signal transferring clockwise ( $a \rightarrow c \rightarrow b \rightarrow a$ ) for  $\theta = 3\pi/2$ . These agree well with the numerical results shown in Fig. 5.

Finally, we discuss the effects of the vacuum noise spectrum  $s_{v,\text{vac}}(\omega)$  given by Eqs. (31)–(33). The vacuum noise spectrum  $s_{v,\text{vac}}(\omega)$  ( $v = a, b, c$ ) as a function of the frequency of the incoming signal  $\omega$  is shown in Fig. 7. The effects of the vacuum noises are so small that they are insignificant even for the input signals of the single-photon (single-phonon) level (about  $2 \times 10^{-3}$  at  $\omega = \omega_m = 10\gamma$ ). The physical origin of the vacuum noise in the output spectrum is the anti-rotating-wave interactions between the optical and mechanical modes

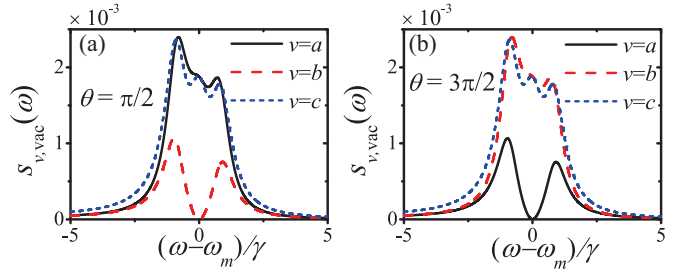


FIG. 7. (Color online) The vacuum noise spectrum  $s_{v,\text{vac}}(\omega)$  ( $v = a, b, c$ ) as a function of the frequency of the incoming signal  $\omega$  for different phase difference: (a)  $\theta = \pi/2$  and (b)  $\theta = 3\pi/2$ . The other parameters are  $\Delta'_a = \Delta'_b = \omega_m = 10\gamma$ ,  $J = G_a = G_b e^{-i\theta} = \gamma_a/2 = \gamma_b/2 = \gamma_m/2 = \gamma/2$ .

[included in Eq. (11)]. The suppression of the vacuum noise for mode  $b$  (mode  $a$ ) at  $\omega = \omega_m$  as  $\theta = \pi/2$  ( $\theta = 3\pi/2$ ) is due to the negligible effect of the anti-rotating-wave interaction between the two optical modes. When all the anti-rotating-wave interactions (between the optical and mechanical modes and between the two optical modes) are neglected, there is no vacuum noise in the output field, as shown in Eqs. (44) and (45).

## V. CONCLUSIONS

In summary, we have shown the optical nonreciprocity in a three-mode optomechanical system. We demonstrated that the nonreciprocal response is enabled by tuning the phase difference between the optomechanical coupling rates to induce the time-reversal-symmetry breaking of the system. Then we showed that the three-mode optomechanical system can also be used as a three-port optomechanical circulator for two optical modes and one mechanical mode. Further, we note that the three-mode optomechanical system can work in the single-photon level and can be integrated into a chip. The three-port optomechanical circulator might eventually provide the basis for applications on quantum information processing or quantum simulation [29].

*Note added.* Recently, we became aware of a related paper by Metelmann and Clerk [30].

## ACKNOWLEDGMENTS

We thank W. H. Hu and L. Ge for fruitful discussions. This work is supported by the Postdoctoral Science Foundation of China (under Grant No. 2014M550019), the National Natural Science Foundation of China (under Grants No. 11422437, No. 11174027, and No. 11121403), and the National Basic Research Program of China (under Grants No. 2012CB922104 and No. 2014CB921403).

[1] R. J. Potton, *Rep. Prog. Phys.* **67**, 717 (2004); I. V. Shadrivov, V. A. Fedotov, D. A. Powell, Y. S. Kivshar, and N. I. Zheludev, *New J. Phys.* **13**, 033025 (2011).

[2] J. Fujita, M. Levy, R. M. Osgood, L. Wilkens, and H. Dötsch, *Appl. Phys. Lett.* **76**, 2158 (2000); R. L. Espinola, T. Izuhara, M. C. Tsai, R. M. Osgood, Jr., and H. Dötsch,

- Opt. Lett.* **29**, 941 (2004); T. R. Zaman, X. Guo, and R. J. Ram, *Appl. Phys. Lett.* **90**, 023514 (2007); F. D. M. Haldane and S. Raghu, *Phys. Rev. Lett.* **100**, 013904 (2008); Y. Shoji, T. Mizumoto, H. Yokoi, I. Hsieh, and R. M. Osgood, *Appl. Phys. Lett.* **92**, 071117 (2008); Z. Wang, Y. Chong, J. D. Joannopoulos, and M. Soljačić, *Nature (London)* **461**, 772 (2009); Y. Hadad and B. Z. Steinberg, *Phys. Rev. Lett.* **105**, 233904 (2010); A. B. Khanikaev, S. H. Mousavi, G. Shvets, and Y. S. Kivshar, *ibid.* **105**, 126804 (2010); L. Bi, J. Hu, P. Jiang, D. H. Kim, G. F. Dionne, L. C. Kimerling, and C. A. Ross, *Nat. Photonics* **5**, 758 (2011); Y. Shoji, M. Ito, Y. Shirato, and T. Mizumoto, *Opt. Express* **20**, 18440 (2012).
- [3] K. Gallo, G. Assanto, K. R. Parameswaran, and M. M. Fejer, *Appl. Phys. Lett.* **79**, 314 (2001); S. F. Mingaleev and Y. S. Kivshar, *J. Opt. Soc. Am. B* **19**, 2241 (2002); M. Soljačić, C. Luo, J. D. Joannopoulos, and S. Fan, *Opt. Lett.* **28**, 637 (2003); A. Rostami, *Opt. Laser Technol.* **39**, 1059 (2007); A. Alberucci and G. Assanto, *Opt. Lett.* **33**, 1641 (2008); L. Fan, J. Wang, L. T. Varghese, H. Shen, B. Niu, Y. Xuan, A. M. Weiner, and M. Qi, *Science* **335**, 447 (2012); L. Fan, L. T. Varghese, J. Wang, Y. Xuan, A. M. Weiner, and M. Qi, *Opt. Lett.* **38**, 1259 (2013); B. Anand, R. Podila, K. Lingam, S. R. Krishnan, S. S. S. Sai, R. Philip, and A. M. Rao, *Nano Lett.* **13**, 5771 (2013).
- [4] F. Biancalana, *J. Appl. Phys.* **104**, 093113 (2008); A. E. Miroshnichenko, E. Brasselet, and Y. S. Kivshar, *Appl. Phys. Lett.* **96**, 063302 (2010); C. Wang, C. Zhou, and Z. Li, *Opt. Express* **19**, 26948 (2011); C. Wang, X.-L. Zhong, and Z.-Y. Li, *Sci. Rep.* **2**, 674 (2012); K. Xia, M. Alamri, and M. S. Zubairy, *Opt. Express* **21**, 25619 (2013); E. J. Lenferink, G. Wei, and N. P. Stern, *ibid.* **22**, 16099 (2014); Y. Yu, Y. Chen, H. Hu, W. Xue, K. Yvind, and J. Mork, *arXiv:1409.3147*.
- [5] Z. F. Yu and S. H. Fan, *Nat. Photonics* **3**, 91 (2009); K. Fang, Z. Yu, and S. Fan, *ibid.* **6**, 782 (2012); E. Li, B. J. Eggleton, K. Fang, and S. Fan, *Nat. Commun.* **5**, 3225 (2014); C. R. Doerr, N. Dupuis, and L. Zhang, *Opt. Lett.* **36**, 4293 (2011); C. R. Doerr, L. Chen, and D. Vermeulen, *Opt. Express* **22**, 4493 (2014); H. Lira, Z. F. Yu, S. H. Fan, and M. Lipson, *Phys. Rev. Lett.* **109**, 033901 (2012); K. Fang, Z. Yu, and S. Fan, *ibid.* **108**, 153901 (2012); M. Castellanos Munoz, A. Y. Petrov, L. O’Faolain, J. Li, T. F. Krauss, and M. Eich, *ibid.* **112**, 053904 (2014); Y. Yang, C. Galland, Y. Liu, K. Tan, R. Ding, Q. Li, K. Bergman, T. Baehr-Jones, and M. Hochberg, *Opt. Express* **22**, 17409 (2014).
- [6] Q. Wang, F. Xu, Z. Y. Yu, X. S. Qian, X. K. Hu, Y. Q. Lu, and H. T. Wang, *Opt. Express* **18**, 7340 (2010); M. S. Kang, A. Butsch, and P. S. J. Russell, *Nat. Photonics* **5**, 549 (2011).
- [7] C. Eütter, K. G. Makris, R. El-Ganainy, D. N. Christodoulides, M. Segev, and D. Kip, *Nat. Phys.* **6**, 192 (2010); H. Ramezani, T. Kottos, R. El-Ganainy, and D. N. Christodoulides, *Phys. Rev. A* **82**, 043803 (2010); L. Feng, M. Ayache, J. Q. Huang, Y. L. Xu, M. H. Lu, Y. F. Chen, Y. Fainman, and A. Scherer, *Science* **333**, 729 (2011); B. Peng, S. K. Özdemir, F. Lei, F. Monifi, M. Gianfreda, G. L. Long, S. H. Fan, F. Nori, C. M. Bender, and L. Yang, *Nat. Phys.* **10**, 394 (2014); J. H. Wu, M. Artoni, and G. C. La Rocca, *Phys. Rev. Lett.* **113**, 123004 (2014).
- [8] D. W. Wang, H. T. Zhou, M. J. Guo, J. X. Zhang, J. Evers, and S. Y. Zhu, *Phys. Rev. Lett.* **110**, 093901 (2013); S. A. R. Horsley, J. H. Wu, M. Artoni, and G. C. La Rocca, *ibid.* **110**, 223602 (2013).
- [9] Y. Shen, M. Bradford, and J. T. Shen, *Phys. Rev. Lett.* **107**, 173902 (2011); K. Xia, G. Lu, G. Lin, Y. Cheng, Y. Niu, S. Gong, and J. Twamley, *Phys. Rev. A* **90**, 043802 (2014); H. Z. Shen, Y. H. Zhou, and X. X. Yi, *ibid.* **90**, 023849 (2014).
- [10] T. J. Kippenberg and K. J. Vahala, *Science* **321**, 1172 (2008); F. Marquardt and S. M. Girvin, *Physics* **2**, 40 (2009); M. Aspelmeyer, P. Meystre, and K. Schwab, *Phys. Today* **65**(7), 29 (2012); M. Aspelmeyer, T. J. Kippenberg, and F. Marquardt, *Rev. Mod. Phys.* **86**, 1391 (2014).
- [11] S. Manipatruni, J. T. Robinson, and M. Lipson, *Phys. Rev. Lett.* **102**, 213903 (2009).
- [12] M. Hafezi and P. Rabl, *Opt. Express* **20**, 7672 (2012).
- [13] M. Ludwig, A. H. Safavi-Naeini, O. Painter, and F. Marquardt, *Phys. Rev. Lett.* **109**, 063601 (2012); K. Stannigel, P. Komar, S. J. M. Habraken, S. D. Bennett, M. D. Lukin, P. Zoller, and P. Rabl, *ibid.* **109**, 013603 (2012).
- [14] Y. D. Wang and A. A. Clerk, *Phys. Rev. Lett.* **108**, 153603 (2012); L. Tian, *ibid.* **108**, 153604 (2012); H. K. Li, X. X. Ren, Y. C. Liu, and Y. F. Xiao, *Phys. Rev. A* **88**, 053850 (2013).
- [15] I. S. Grudinin, H. Lee, O. Painter, and K. J. Vahala, *Phys. Rev. Lett.* **104**, 083901 (2010); H. Wang, Z. X. Wang, J. Zhang, S. K. Özdemir, L. Yang, and Y. X. Liu, *Phys. Rev. A* **90**, 053814 (2014).
- [16] W. J. Gu and G. X. Li, *Phys. Rev. A* **87**, 025804 (2013); T. Ojanen and K. Børkje, *ibid.* **90**, 013824 (2014); Y. J. Guo, K. Li, W. J. Nie, and Y. Li, *ibid.* **90**, 053841 (2014); Y. C. Liu, Y. F. Xiao, X. S. Luan, Q. H. Gong, and C. W. Wong, *ibid.* **91**, 033818 (2015).
- [17] X. W. Xu and Y. J. Li, *J. Opt. B* **46**, 035502 (2013); V. Savona, *arXiv:1302.5937*.
- [18] J. Koch, A. A. Houck, K. L. Hur, and S. M. Girvin, *Phys. Rev. A* **82**, 043811 (2010).
- [19] S. J. M. Habraken, K. Stannigel, M. D. Lukin, P. Zoller, and P. Rabl, *New J. Phys.* **14**, 115004 (2012).
- [20] J. D. Thompson, B. M. Zwickl, A. M. Jayich, F. Marquardt, S. M. Girvin, and J. G. E. Harris, *Nature (London)* **452**, 72 (2008); G. Heinrich, J. G. E. Harris, and F. Marquardt, *Phys. Rev. A* **81**, 011801(R) (2010); H. Z. Wu, G. Heinrich, and F. Marquardt, *New J. Phys.* **15**, 123022 (2013).
- [21] Q. Lin, J. Rosenberg, X. Jiang, K. J. Vahala, and O. Painter, *Phys. Rev. Lett.* **103**, 103601 (2009); M. Li, W. H. P. Pernice, and H. X. Tang, *Nat. Photonics* **3**, 464 (2009); S. Weis, R. Rivière, S. Deléglise, E. Gavartin, O. Arcizet, A. Schliesser, and T. J. Kippenberg, *Science* **330**, 1520 (2010).
- [22] M. Eichenfield, R. Camacho, J. Chan, K. J. Vahala, and O. Painter, *Nature (London)* **459**, 550 (2009); A. H. Safavi-Naeini and O. Painter, *Opt. Express* **18**, 14926 (2010); J. T. Hill, A. H. Safavi-Naeini, J. Chan, and O. Painter, *Nat. Commun.* **3**, 1196 (2012); A. H. Safavi-Naeini, J. T. Hill, S. Meenehan, J. Chan, S. Gröblacher, and O. Painter, *Phys. Rev. Lett.* **112**, 153603 (2014).
- [23] J. D. Teufel, D. Li, M. S. Allman, K. Cicak, A. J. Sirois, J. D. Whittaker, and R. W. Simmonds, *Nature (London)* **471**, 204 (2011); F. Massel, S. Un Cho, J.-M. Pirkkalainen, P. J. Hakonen, T. T. Heikkilä, and M. A. Sillanpää, *Nat. Commun.* **3**, 987 (2012); T. A. Palomaki, J. D. Teufel, R. W. Simmonds, and K. W. Lehnert, *Science* **342**, 710 (2013); J. Suh, A. J. Weinstein, C. U. Lei, E. E. Wollman, S. K. Steinke, P. Meystre, A. A. Clerk, and K. C. Schwab, *ibid.* **344**, 1262 (2014).
- [24] E. X. DeJesus and C. Kaufman, *Phys. Rev. A* **35**, 5288 (1987); I. S. Gradshteyn and I. M. Ryzhik, in *Table of Integrals, Series and Products* (Academic, Orlando, 1980), p. 1119; M. Paternostro, S. Gigan, M. S. Kim, F. Blaser, H. R. Böhm, and

- M. Aspelmeyer, *New J. Phys.* **8**, 107 (2006); D. Vitali, S. Gigan, A. Ferreira, H. R. Böhm, P. Tombesi, A. Guerreiro, V. Vedral, A. Zeilinger, and M. Aspelmeyer, *Phys. Rev. Lett.* **98**, 030405 (2007); R. Ghobadi, A. R. Bahrampour, and C. Simon, *Phys. Rev. A* **84**, 033846 (2011).
- [25] C. W. Gardiner and M. J. Collett, *Phys. Rev. A* **31**, 3761 (1985).
- [26] G. S. Agarwal and S. Huang, *Phys. Rev. A* **85**, 021801(R) (2012).
- [27] R. H. Olsson, III, and I. El-Kady, *Meas. Sci. Technol.* **20**, 012002 (2009); M. Maldovan, *Nature (London)* **503**, 209 (2013).
- [28] A. H. Safavi-Naeini and O. Painter, *New J. Phys.* **13**, 013017 (2011).
- [29] A. Nunnenkamp, J. Koch, and S. M. Girvin, *New J. Phys.* **13**, 095008 (2011); A. L. C. Hayward, A. M. Martin, and A. D. Greentree, *Phys. Rev. Lett.* **108**, 223602 (2012); R. O. Umucalilar and I. Carusotto, *ibid.* **108**, 206809 (2012); I. M. Georgescu, S. Ashhab, and F. Nori, *Rev. Mod. Phys.* **86**, 153 (2014).
- [30] A. Metelmann and A. A. Clerk, [arXiv:1502.07274](https://arxiv.org/abs/1502.07274).